Himmelfarb Health Sciences Library, The George Washington University
Health Sciences Research Commons

11-17-2017

Transcriptional Alterations in Hereditary and Sporadic Nonfunctioning Pancreatic Neuroendocrine Tumors According to Genotype.

Xavier M Keutgen

Suresh Kumar

Sudheer Gara

Myriem Boufraqech

Sunita Agarwal

See next page for additional authors

APA Citation

Authors

Xavier M Keutgen, Suresh Kumar, Sudheer Gara, Myriem Boufraqech, Sunita Agarwal, Ralph H Hruban, Naris Nilubol, Martha Quezado, Richard Finney, Maggie Cam, and Electron Kebebew

Original Article

Transcriptional Alterations in Hereditary and Sporadic Nonfunctioning Pancreatic Neuroendocrine Tumors According to Genotype

Xavier M. Keutgen, MD [ID][1,2]; Suresh Kumar, PhD[1]; Sudheer Gara, PhD[1]; Myriem Boufraqech, PhD[1]; Sunita Agarwal, MD[3]; Ralph H. Hruban, MD[4]; Naris Nilubol, MD[1]; Martha Quezado, MD[5]; Richard Finney, PhD[6]; Maggie Cam, PhD[6]; and Electron Kebebew, MD [ID][1,7]

BACKGROUND: Nonfunctioning pancreatic neuroendocrine tumors (NFPanNETs) may be sporadic or inherited because of germline mutations associated with von Hippel-Lindau disease (VHL) or multiple endocrine neoplasia type 1 (MEN1). The clinical behavior of NFPanNETs is difficult to predict, even in tumors of the same stage and grade. The authors analyzed genotype-specific patterns of transcriptional messenger RNA (mRNA) levels of NFPanNETs to understand the molecular features that determine PanNET pheno-type. **METHODS:** Thirty-two samples were included for genome-wide mRNA gene expression analysis (9 VHL-associated, 10 MEN1-associated, and 9 sporadic NFPanNETs and 4 purified normal islet cell [NIC] samples). Validation of genes was performed by real-time polymerase chain reaction analysis and immunohistochemistry. Gene expression profiles were analyzed by tumor genotype, and pathway analysis was curated. **RESULTS:** Consensus clustering of mRNA expression revealed separate clustering of NICs, VHL-associated NFPanNETs, and MEN1-associated NFPanNETs; whereas some sporadic tumors clustered with MEN1. Four of 5 MEN1-like sporadic PanNET subtypes had loss of heterozygosity at the *MEN1* gene locus. Pathway analysis demonstrated subtype-specific path-way activation, comprising angiogenesis and immune response in VHL; neuronal development in MEN1; protein ubiquitination in the new MEN1/sporadic subtype; and cytokinesis and cilium/microtubule development in sporadic NFPanNETs. Among many genes, platelet-derived growth factor receptor β (PDGFRB), lymphoid enhancer-binding factor-1 (Lef-1), cyclin-dependent kinase 4 (CDK4), and CDK6 were upregulated in VHL or MEN1 NFPanNETs, providing potential subtype-specific treatment targets. **CONCLUSIONS:** Distinct mRNA expression patterns were identified in sporadic-associated, VHL-associated, and MEN1-associated NFPanNETs. The current results uncover new pathways involved in NFPanNETs that are subtype-specific and provide potential new diagnostic or therapeutic targets based on tumor subtype. *Cancer* 2017;000:000-000. © 2017 American Cancer Society.

KEYWORDS: multiple endocrine neoplasia type 1 (MEN1), neuroendocrine, pancreas, sporadic, von Hippel-Lindau syndrome (VHL).

INTRODUCTION

Pancreatic neuroendocrine tumors (PanNETs) are characterized by a distinctive histology and evidence of neuroendocrine differentiation. In the United States, it is estimated that 3 to 5 cases per 100,000 inhabitants occur annually, and the incidence of these neoplasms continues to increase.[1] PanNETs can be divided into functioning tumors (produce clinical findings related to excess hormone production) and nonfunctioning tumors (NFPanNETs), and the latter are much more prevalent. Although functioning PanNETs require treatment because of the morbidity and mortality caused by excess hormone production, small NFPanNETs do not always require treatment.

PanNETs can occur sporadically or in inherited cancer syndromes, such as von Hippel-Lindau syndrome (VHL), multiple endocrine neoplasia type 1 (MEN1), neurofibromatosis type 1 (NF1), tuberous sclerosis complex (TSC), and Cowden syndrome (CS).[2-6] From 9% to 17% of patients with VHL and from 30% to 80% of patients with MEN1 develop PanNETs during their lifetime.[4,7] By contrast, the penetrance of PanNETs in NF1, TSC, and CS is lower; and these latter syndromes are relatively rare.

Hereditary PanNETs often behave less aggressively than their sporadic counterparts, but the reasons underlying these differences in clinical behavior are not well defined.[4,8] The clinical management of hereditary PanNETs is complicated by the presence of multiple lesions and the risks associated with multiple surgeries. Current recommendations for resection of hereditary PanNETs are mostly based on the risk of metastatic disease, using tumor growth and size as surrogate markers for aggressiveness.[4,7] However, these criteria are imperfect and do not accurately predict the metastatic potential and/or aggressive behavior of all patients with PanNETs and VHL or MEN1.[7,9-12]

The genes responsible for the major inherited predisposition syndromes (*VHL, MEN1*) are known, and large numbers of PanNETs have been sequenced.[13] Sequencing of sporadic PanNETs have identified a multitude of somatic mutations, including *MEN1* in up to 44% of cases and death domain-associated protein (*DAXX*), α-thalassemia X-linked intellectual disability syndrome (*ATRX*), phosphatase and tensin homolog (*PTEN*), *TSC2*, and phosphatidylinositol 4,5-bisphosphate 3-kinase catalytic subunit α (*PIK3CA*), as well as mutations or promoter hypermethylation in *VHL* in up to 25% of patients.[13-16] Despite these advances, the transcriptional changes and downstream pathway activations promoting early tumorigenesis are largely unknown but could be useful to identify targets for diagnosis and treatment of both hereditary and sporadic PanNETs.[4,7,17]

In this study, we sought to investigate transcriptional levels of messenger RNA (mRNA) by DNA microarray from hereditary (MEN1, VHL) and sporadic, early stage NFPanNETs to discover dysregulated pathways associated with tumorigenesis and to elucidate possible transcriptional targets that may be deregulated across all genotypes or in just 1 particular genotype of NFPanNETs.

MATERIAL AND METHODS
Sample Selection
Thirty NFPanNETs and 6 normal islet cell (NIC) samples were initially selected for this study. All tumors were chosen to be early stage NFPanNETs to account for stage mismatch when comparing genotypes and to reflect actual, common presentations of NFPanNETs in patients with MEN1 and VHL. Thirty-two samples were ultimately included in this analysis; 1 sporadic sample was excluded because of advanced stage, including metastatic disease; and 1 VHL and 2 NIC samples were excluded because of poor RNA quality. The final analyzed group comprised 10 NFPanNETs from patients with MEN1, 9 NFPanNETs from patients with VHL, 9 sporadic NFPanNETs, and 4 purified NIC samples (Fig. 1). All patients who had MEN1 and VHL had a germline mutation in the respective syndromal gene. The functional status of the tumor was determined by clinical features and symptoms and through biochemical testing (fasting gastrin, insulin, vasoactive intestinal peptide, somatostatin, and glucagon). Immunohistochemistry staining of paraffin-embedded tumor slides for gastrin and insulin also was performed in MEN1-associated NFPanNETs. Tissues were obtained from pancreatectomies (pancreaticoduodenectomy or distal pancreatectomy specimens) or NFPanNET enucleations performed at our hospital or at the participating institution between 2010 and 2014. These samples were fresh-frozen after procurement and stored at −80 °C. Serial tissue sections were used for RNA extraction, stained with hematoxylin and eosin, and reviewed by a pathologist to confirm the diagnosis and ensure that the section had >80% neoplastic nuclei content.

Primary human pancreatic islets of Langerhans were purchased from the Division of Transplantation Surgery at the University of Alabama at Birmingham. Pancreata were recovered, with informed consent, from cadaveric donors after in situ vascular perfusion with University of Wisconsin solution at 4 °C as part of a multiorgan procurement. Pancreata were immediately transported to the islet isolation laboratory for processing. Islets were isolated using a semiautomated method and were purified using the Cobe 2991 cell processor (Gambro BCT, Lakewood, CO). The number of islets within each size class was converted to the standard number of islets measuring 150 μm in greatest dimension (equal in volume to the sample). Purity was assessed by comparing the relative quantity of dithiozone-stained endocrine tissue with that of unstained exocrine tissue. Only islet isolations with >90% viability and >60% purity were used.

This study was approved by the Office for Human Research Protections at the Department of Health and Human Services. Patient information was collected prospectively under an Institutional Review Board-approved protocol at the National Institutes of Health (Bethesda, MD) after obtaining written informed consent.

RNA Extraction
Total RNA was extracted from approximately 20 to 30 mg of tissue using the Total RNA Purification Kit (17200; Norgen Biotek Corporation, Thorold, ON, Canada) and from purified NICs using the AllPrep DNA/RNA Mini Kit (catalog no. 80204; Qiagen,

Hilden, Germany). Total RNA yield was assessed using NanoDrop (NanoDrop Technologies, Wilmington, DE) and the Bioanalyzer 2100 and RNA 6000 Nano/Pico LabChip (Agilent Technologies, Palo Alto, CA). Complementary DNA (cDNA) was obtained by reverse transcription using the Murine Leukemia Virus Reverse Transcriptase (M-MLV RT) protocol (Thermo Fisher Scientific, Waltham, MA).

Messenger RNA microarray
Samples
RNA quantity and quality were measured using the NanoDrop ND-1000 spectrophotometer (NanoDrop Technologies). RNA integrity was assessed by standard denaturing agarose gel electrophoresis.
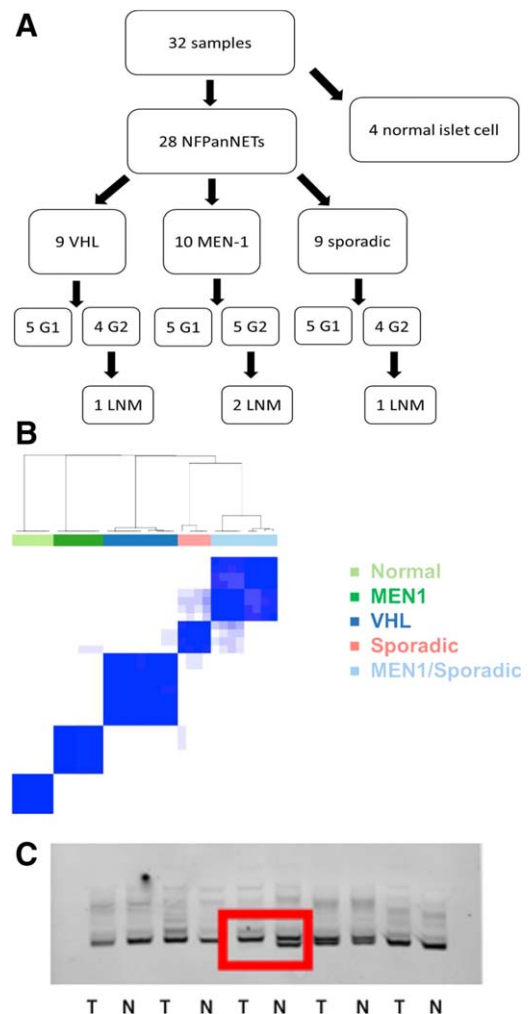
DNA microarray
The Whole Human Genome Oligo Microarray (Agilent Technologies) provides a broad view that represents all known genes and transcripts in the human genome. Sequences were compiled from a broad-source survey and then verified and optimized by alignment to the assembled human genome.

RNA labeling and array hybridization
Sample labeling and array hybridization were performed according to the Agilent One-Color Microarray-Based Gene Expression Analysis protocol (Agilent Technologies). Briefly, total RNA from each sample was linearly amplified and labeled with indocarbocyanine (Cy3)-uridine diphosphate. The labeled complementary RNAs (cRNAs) were purified using the RNeasy Mini Kit (Qiagen). The concentration and specific activity of the labeled cRNAs (pmol Cy3/µg cRNA) were measured using the NanoDrop ND-1000 spectrophotometer. One microgram of each labeled cRNA was fragmented by adding 11 µL 10 × blocking agent and 2.2 µL 25 × fragmentation buffer; heating at 60 °C for 30 minutes; and finally adding 55 µL 2 × gene expression hybridization buffer to dilute the labeled cRNA. One hundred microliters of hybridization solution was dispensed into the gasket slide and assembled to the gene expression microarray slide. The slides were incubated for 17 hours at 65 °C in an Agilent hybridization oven (Agilent Technologies). The hybridized arrays were then washed, fixed, and scanned using the Agilent DNA Microarray Scanner (part number G2505C; Agilent Technologies).

Data analysis
Agilent Feature Extraction software (version 11.0.1.1; Agilent Technologies) was used to analyze the acquired

Figure 1. (A) This is a breakdown of nonfunctioning pancreatic neuroendocrine tumors (NFPanNETs) and normal islet cell samples analyzed by complementary DNA microarray. G indicates grade; LNM, lymph node metastases; MEN-1, multiple endocrine neoplasia type 1; VHL, von Hippel-Lindau disease. (B) Unsupervised hierarchical clustering of microarray data defines 5 distinct groups. (C) This is a representative image of loss of heterozygosity for the MEN1 gene in a sporadic NFPanNET using the microsatellite marker DS11S956 (red box). T indicates tumor; N, normal.

array images. Quantile normalization and subsequent data processing were performed using GeneSpring GX software (version 12.1; Agilent Technologies). Raw data were normalized using quantile normalization, followed by cyclic loess using the Bioconductor limma package (version 3.30.11; Bioconductor Core Team, Roswell Park Cancer Institute, Buffalo, NY).[18] Consensus clustering was performed on all gene expression data using the Bioconductor package ConsensusClusterPlus (version 1.38; Bioconductor Core Team).[19] We evaluated from k = 2 to 6 clusters and selected k = 5 clusters that had the

maximum area under the curve in the consensus cumulative distribution function plot. Subtype-unique expressed genes were identified by selecting genes, wherein the 90% confidence interval (CI) within each subtype exceeded the 90% CI of expression for all other subtypes, including normal. Subtype-unique gene lists were subjected to gene category enrichment analysis using the Fisher exact test on various publicly available databases, including Gene Ontology (GO) (https://www.geneontology.org, Accessed May 1, 2017), Kyoto Encyclopedia of Genes and Genomes (KEGG) (https://www.genome.jp/kegg/pathway.html, Accessed May 1, 2017), Protein Analysis Through Evolutionary Relationships (PANTHER) (https://www.pantherdb.org, Accessed May 1, 2017), PC REACTOME (https://www.reactome.org, Accessed May 1, 2017), Inter Partes Review (IPR), PC NCI NATURE (http://pid.nci.nih.gov, Accessed May 1, 2017), and the National Center for Biotechnology Information (https://www.ncbi.nlm.nih.gov, Accessed May 1, 2017) database.

Group comparisons of categorical variables were performed using the Pearson chi-square test or the Fisher exact probability test, and the comparison of continuous variables was performed with 2-tailed t tests or Wilcoxon rank tests. All P values were considered statistically significant if P was less than .05. GraphPad Prism (GraphPad Software Inc, La Jolla, CA) was used for statistical analyses.

Ion Torrent Next-Generation Sequencing Analysis

Primers for the genes involved in NFPanNETs (*MEN1, ATRX, DAXX*, and *VHL*) were designed for a custom Ampliseq panel using Life Technologies software (Ion Ampliseq Designer; Thermo Fisher Scientific). Ampliseq libraries were prepared from DNA samples extracted from NFPanNET samples using the RNA/DNA/Protein Purification Plus Kit (47700; Norgen Biotek Corporation). DNA sample concentrations were determined using NanoDrop (ND8000; Thermo Fisher Scientific). Final sample qualification and quantification were established with Picogreen analysis (standard curve assay) on a Molecular Devices Gemini XPS Plate Reader and Softmax Pro Software (Molecular Devices, Sunnyvale, CA). All samples and controls were run in triplicate.

Ampliseq libraries were prepared for each DNA sample. To create libraries, each DNA sample was first amplified according to the manufacturer's protocol. Each library was then assigned a unique, barcode-adapter sequence and ligated onto the libraries. The final libraries were qualified and quantified using Life Technologies' Ion Library Quantitation Kit (item 4468802; Thermo Fisher Scientific).

Libraries were then cycled and analyzed on an ABI PRISM 7900HT Sequence Detection System (Thermo Fisher Scientific). By using the quantification values from the real-time polymerase chain reaction (PCR) analysis, all libraries were then normalized with 1X low Tris-ethylenediaminetetraacetic acid buffer to either 50 or 100 pMol to prepare for emulsion PCR. Libraries were then combined into pools of 9 for a total of 4 pools. Combined with an Ion 318 chip, roughly 300X coverage per amplicon was achieved. The clonal emulsion amplification of Ampliseq libraries was sequenced on the Ion Torrent Personal Genome Machine (PGM) platform using the Life Technologies OneTouch 2 (OT2) system (Thermo Fisher Scientific). The OT2 system is automated and, when used in conjunction with the Enrichment Station, generates template-positive, Ion PGM Template OT2 200 Ion Sphere Particles for semiconductor sequencing. All analyses and data quality controls were completed using the Life Technologies Ion Torrent Suite (version 5.0.4).

Real-Time PCR

Gene expression levels were measured using specific primers and probes. Briefly, 500 to 1000 ng of total RNA was reverse transcribed using a High-Capacity Reverse Transcription cDNA Kit (catalog no. 4374967; Applied Biosystems, Thermo Fisher Scientific), and the resulting cDNA was diluted and amplified according to the manufacturer's instructions. Glyceraldehyde 3-phosphate dehydrogenase was used as an endogenous control. Gene expression levels were calculated using SDS 2.3 software (Applied Biosystems, Thermo Fisher Scientific).

Immunohistochemistry

Sections were deparaffinized and rehydrated, and antigen retrieval was performed with citrate buffer in a water bath at 120 °C. The sections were incubated with the anti-platelet-derived growth factor receptor β (anti-PDGFRB) antibody (1:100 dilution; Abcam, Cambridge, UK) overnight at 4 °C, followed by incubation with a biotinylated secondary antibody for 1 hour at room temperature. The slides were developed with diaminobenzidine (EnVision Kit System Horseradish Peroxidase [diaminobenzidine]; Dako, Carpinteria, CA) and counterstained with hematoxylin. Then, the slides were scanned at ×20 magnification using a ScanScope XT digital slide scanner (Aperio Technologies, Leica Biosystems Nussloch, GmbH, Nussloch, Germany) to create whole-slide image data files at a resolution of 0.5 mm/pixel and viewed using ImageScope software (Aperio Technologies). All immunohistochemistry slides were reviewed and scored by a pathologist who

was unaware of the sample groups. Tumor staining in > 50% of each slide was considered positive. Positive staining was graded as weakly positive (+), moderately positive (++), or strongly positive (+++).

DNA Extraction and Loss of Heterozygosity Analysis

DNA was extracted from tissue and leukocytes using the Qiagen Blood and Cell Culture DNA Kit (Qiagen) following the manufacturer's protocol. Primers for the polymorphic microsatellite markers D11S956, D11S4939, D11S4946, PYGM, and D11S987 were identical to those published previously.[20] PCR was performed in a total volume of 100 mL containing 30 pmol of each primer, 2.5 U Taq polymerase (Perkin Elmer, Foster City, CA), and 100 to 400 ng DNA. The cycler program was as follows: initial denaturation at 95 °C for 5 minutes; 30 cycles at 55 °C for 1.5 minutes, 72 °C for 1.5 minutes, and 94 °C for 1.5 minutes; and a final extension at 72 °C for 5 minutes. Primer sequences for D11S956, D11S4939, D11S4946, PYGM (glycogen phosphorylase, muscle associated), and D11S987 PCR conditions were used as published previously with minor modifications.[21] The PCR product was purified with chloroform. Purified PCR product was dried in a SpeedVac (Thermo Fisher Scientific), redissolved in 10 μL formamide and 10 μL H_2O, and loaded onto a 6% Tris-borate-ethylenediaminetetraacetic acid polyacrylamide gel. Electrophoresis was performed at 150 V for 90 minutes. After staining with ethidium bromide for 10 minutes, the amplification products were observed on an ultraviolet transilluminator. Loss of heterozygosity (LOH) was determined by comparing tumor DNA versus the germline DNA pattern.

RESULTS

Histopathologic Characteristics

Twenty-eight patient samples with NFPanNETs were selected according to the criteria described above (see Materials and Methods). Fifty percent of samples were World Health Organization grade 1 tumors, and 50% were World Health Organization grade 2 tumors in each subgroup (VHL, MEN1, and sporadic). Two patients in the VHL group and 1 patient in the MEN1 and sporadic group had lymph node metastases at the time of diagnosis. There were no statistically significant differences when comparing clinical and histopathologic characteristics between subgroups, except for tumor size, which was significantly larger in sporadic tumors compared with VHL (P = .01) and MEN1

NFPanNET samples (P = .002) (Fig. 1A, Supporting Table 1; see online supporting information).

Consensus cluster analysis

Consensus cluster analysis of gene expression levels revealed that NICs and VHL tumor samples clustered in separate groups, whereas sporadic and MEN1 samples clustered alone or in a fifth MEN1/sporadic group (Fig. 1B). We did not observed any clustering according to patient demographic or histopathologic data or MEN1 mutation locus between the MEN1, sporadic, and MEN1/sporadic groups. Ion Torrent next-generation sequencing analysis identified 2 nonsynonymous and 1 stop-gain exonic mutations in *MEN1* in 3 separate sporadic NFPanNET samples that clustered with the MEN1 group; and LOH analysis revealed LOH at the *MEN1* locus in 4 of 5 samples (Fig. 1C), possibly explaining why these samples clustered into the fifth group on unsupervised cluster analysis and confirming the common occurrence of *MEN1* mutations in sporadic PanNETs, as previously reported.[13] Because it was reported previously that the transcription/chromatin remodeling genes *DAXX* (death-domain-associated protein) and *ATRX* were commonly mutated in NFPanNETs,[13] we evaluated whether somatic mutation in these genes influenced transcriptional clustering. Four *ATRX* mutations no *DAXX* mutations were identified in MEN1 and sporadic NFPanNET samples. Two nonsynonymous exonic *ATRX* mutations were identified in the sporadic only group, including 1 nonsynonymous exonic mutation in the MEN1/sporadic group and 1 nonsynonymous exonic mutation in the MEN1 group, suggesting that *ATRX* and *DAXX* mutations were not associated with the transcriptional clustering of tumor samples.

Differentially expressed genes in NFPanNETs according to genotype

A limited list of the most highly upregulated genes in NFPanNETs according to subtype is summarized in Supporting Figure 1 (see online supporting information). The most commonly upregulated genes in all 3 subtypes compared with NICs was Kruppel-like factor 12 (KLF12). *KLF12* is a developmentally regulated transcription factor that has demonstrated the ability to promote cell-cycle transition and regulate anoikis through S-phase and, thus, regulate cell proliferation. It was the gene with the highest predicted connectivity in a recent study evaluating integrated mRNA-microRNA analysis in PanNETs.[22,23] We randomly selected 2 overexpressed genes (KLF-12 and cyclin D1 binding protein 1 [CCNDBP1]), and 1 under expressed gene (matrix metallopeptidase

1 [MMP1]) for validation by reverse transcriptase-quantitative PCR (Supporting Fig. 2; see online supporting information).

We also observed genotype-specific differences in gene expression when we compared 1 subgroup with all others (Supporting Fig. 1; see online supporting information). In the VHL group, we observed overexpression of the neurogenic locus notch homolog protein 3 mRNA (Notch 3), which reportedly is upregulated in the vascular endothelium of VHL-associated central nervous system hemangioblastomas, as well as overexpression of insulin-like growth factor 2 (IGF-2) mRNA, which reportedly is upregulated in the PanNET cell lines BON-1 and QPG-1.[24,25] In the MEN1 group, it was common to observe the overexpression of ryanodine receptor 3 (RYR3) mRNA, which reportedly plays an important role in pancreatic β-cell insulin secretion.[26] It is noteworthy that fibroblast growth factor 13 (FGF-13), which has been associated with aggressive tumor behavior and shorter disease-free survival, was significantly upregulated in the sporadic and MEN1 subgroups only.[27]

GO Pathway Analysis
GO pathway analysis yielded subtype-specific pathway alterations. Among the 20 most upregulated pathways in

VHL-associated NFPanNETs, those relating to angiogenesis and immune response were identified as highly upregulated (Fig. 2). The pathways involved in cilium and microtubule formation, both of which are part of the cell's spindle-cell apparatus and are crucial to cell division, were upregulated in sporadic NFPanNETs, which could explain the reported aggressive behavior and rapid growth of sporadic tumors compared with their hereditary counterparts (Fig. 3).[28] Gene enrichment in pathways comprising ion channel activity and neuron development, both of which reportedly are upregulated in PanNETs, were most prevalent in MEN1-associated NFPanNETs only (Fig. 4).[29] Protein ubiquitination pathways, which reportedly are involved in blockade of the proteasome-degradation machinery and thus enhance glucose-stimulated insulin secretion and promote certain gene-expression patterns, were upregulated most in the MEN1/sporadic NFPanNET subtype (Fig. 5).[30]

Validation of selected genotype-specific mRNA targets
To further validate our microarray analysis, we compared our expression data with results from a previous study that compared mRNA expression in VHL PanNETs with that in sporadic PanNETs.[31] Nineteen genes previously
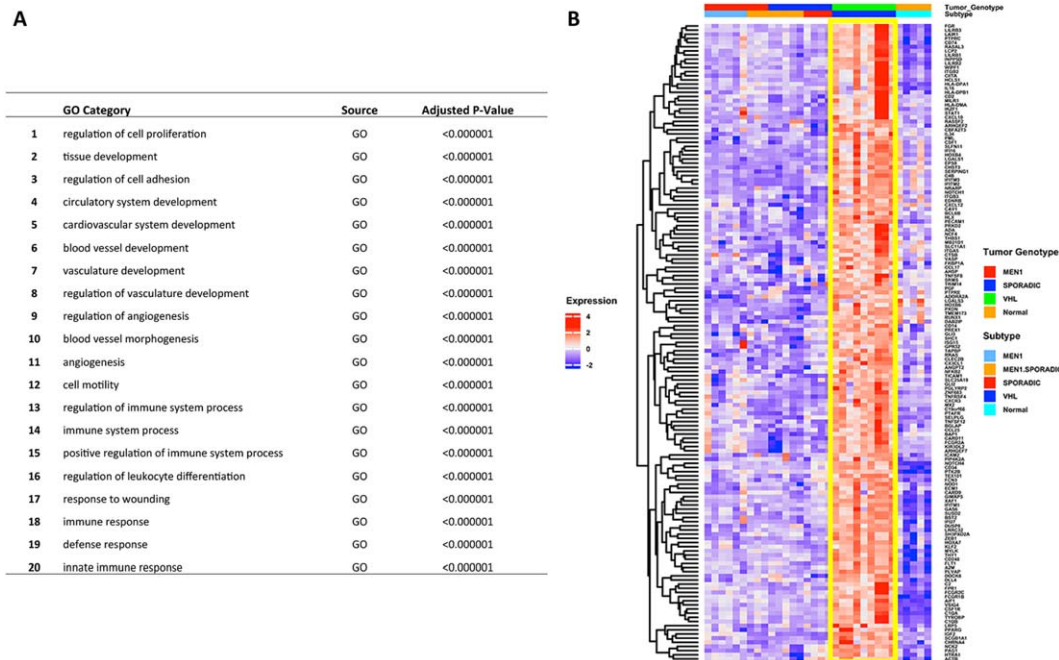
Figure 2. (A) Messenger RNA enrichment analysis (GO, Gene Ontology [GO]) is illustrated for the top 20 upregulated pathways in von Hippel-Lindau disease (VHL) versus other nonfunctioning pancreatic neuroendocrine tumors and normal islet cells. (B) There is a predominance of genes involved in angiogenesis and immune response (yellow box). MEN1 indicates multiple endocrine neoplasia type 1; VHL, von Hippel-Lindau disease.

A

	GO Category	Source	Adjusted P-Value
1	cilium movement	GO	0.00000
2	epithelial cilium movement involved in determination of left/right asymmetry	GO	0.00000
3	axoneme assembly	GO	0.00000
4	microtubule bundle formation	GO	0.00000
5	immune system process	GO	0.00001
6	cilium assembly	GO	0.00001
7	epithelial cilium movement	GO	0.00001
8	cilium organization	GO	0.00002
9	cilium	GO	0.00002
10	Signal Transduction	REACTOME	0.00002
11	immune response	GO	0.00003
12	regulation of intracellular signal transduction	GO	0.00003
13	axonemal dynein complex assembly	GO	0.00003
14	outer dynein arm assembly	GO	0.00009
15	RNA metabolic process	GO	0.00014
16	extracellular region	GO	0.00016
17	G-protein coupled receptor signaling pathway	GO	0.00019
18	regulation of immune system process	GO	0.00020
19	microtubule-based process	GO	0.00020
20	axoneme	GO	0.00022

Figure 3. (A) Messenger RNA enrichment analysis (REACTOME and Gene Ontology [GO]) is illustrated for the top 20 upregulated pathways in sporadic versus other nonfunctioning pancreatic neuroendocrine tumors and normal islet cells. (B) There is a predominance of genes involved in cilium and microtubule processes (yellow box). MEN1 indicates multiple endocrine neoplasia type 1; VHL, von Hippel-Lindau disease.

A

	GO Category	Source	Adjusted P-Value
1	ligand-gated cation channel activity	GO	0.00002
2	behavior	GO	0.00002
3	ligand-gated ion channel activity	GO	0.00018
4	ligand-gated channel activity	GO	0.00018
5	neuron migration	GO	0.00041
6	single-organism behavior	GO	0.00050
7	axon	GO	0.00051
8	gated channel activity	GO	0.00057
9	channel activity	GO	0.00062
10	passive transmembrane transporter activity	GO	0.00063
11	neuron part	GO	0.00065
12	cation channel activity	GO	0.00082
13	nervous system development	GO	0.00093
14	substrate-specific channel activity	GO	0.00112
15	generation of neurons	GO	0.00119
16	neuron projection	GO	0.00124
17	calcium channel activity	GO	0.00251
18	ion channel activity	GO	0.00260
19	divalent inorganic cation transmembrane transporter activity	GO	0.00273
20	neurogenesis	GO	0.00273

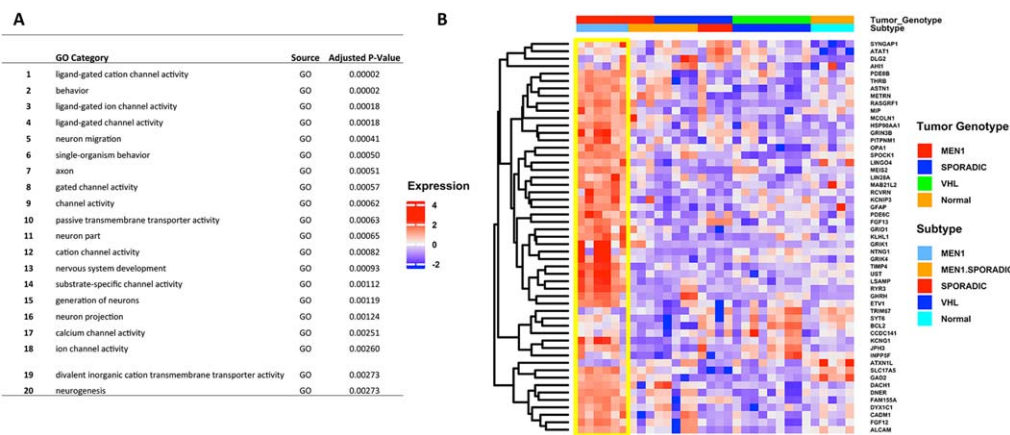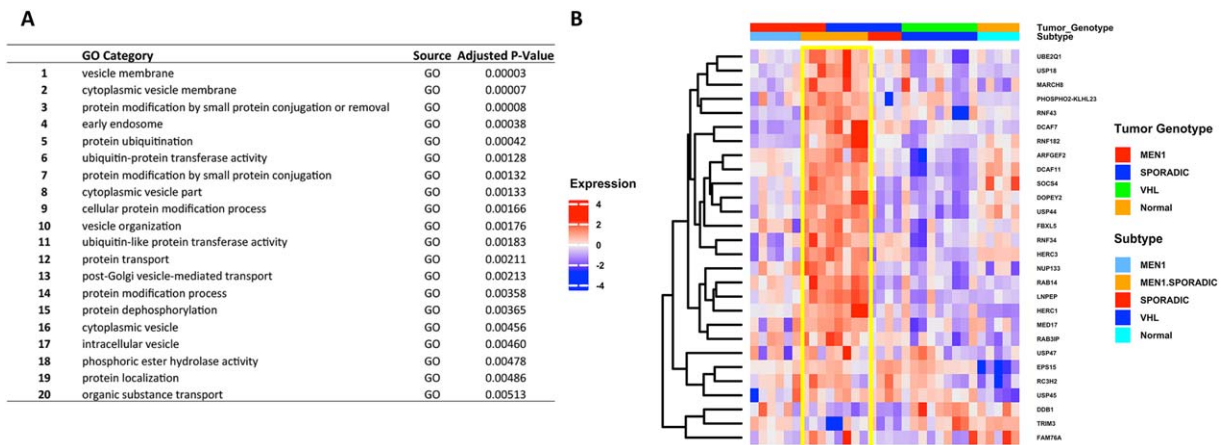
Figure 4. (A) Messenger RNA enrichment analysis (Gene Ontology [GO]) is illustrated for the top 20 upregulated pathways in multiple endocrine neoplasia type 1 (MEN1) versus other nonfunctioning pancreatic neuroendocrine tumors and normal islet cells. (B) There is a predominance of genes involved in ion channel activity and neural development (yellow box). VHL indicates von Hippel-Lindau disease.

reported as upregulated and 3 genes previously reported as downregulated had similar expression levels in our data set when comparing VHL versus sporadic NFPanNETs (Supporting Fig. 3; see online supporting information).

Next, we selected a small subset of genotype-specific genes for validation based on their potential translational relevance because of their ability to be targeted for treatment. We observed that PDGFRB was upregulated (>2-fold) in VHL PanNETs, and this was confirmed by TaqMan reverse transcriptase-PCR (Fig. 6B,C). Immunohistochemical analysis demonstrated that PDGFRB was significantly overexpressed

Figure 5. (A) Messenger RNA enrichment analysis (Gene Ontology [GO]) is illustrated for the top 20 upregulated pathways in multiple endocrine neoplasia type 1(MEN1)/sporadic versus other nonfunctioning pancreatic neuroendocrine tumors and normal islet cells. (B) There is a predominance of genes involved in protein ubiquitination (yellow box). VHL indicates von Hippel-Lindau disease.

in VHL NFPanNETs versus MEN1 and sporadic NFPanNETs ($P = .03$); however, we noted that mostly the tumor stroma, and not the tumor cells, stained positive in VHL samples (Fig. 6A). To test the hypothesis that VHL NFPanNETs have greater stromal content than other PanNETs, we used the Estimation of Stromal and Immune Cells in Malignant Tumors Using Expression Data (ESTIMATE) gene signature model as previously described.[32] We observed significant overexpression of the 141 stromal gene signature panel in VHL tumors compared with the MEN1 and sporadic NFPanNET genotype ($P < .05$) (Fig. 6D).

Additional genes that were upregulated on gene expression analysis and validated by reverse transcriptase-PCR included overexpression of the transcription factor lymphoid enhancer-binding factor-1 (*Lef-1*) in VHL NFPanNETs and overexpression of cyclin-dependent kinase 4 (*CDK4*) and *CDK6* in MEN1 NFPanNETs (Fig. 6E,G,H). The tumor-suppressor *CDKN1B* also was downregulated in MEN1 NFPanNETs compared with other genotypes (Fig. 6F). *CDK4* and *CDK6* gene expression analysis according to groups from hierarchical clustering indicated that *CDK4* levels were higher in the MEN1 and MEN1/sporadic genotypes compared with the sporadic, non-MEN1 genotype, although the difference was not statistically significant (Supporting Fig. 4; see online supporting information).

Next, we evaluated the differentially expressed genes in an independent cohort of previously analyzed PanNETs using publicly available microarray data from the National Center for Biotechnology Information Gene Expression Omnibus (GEO) repository (https://www.ncbi.nlm.nih.gov/geo, Accessed May 1, 2017). In a previously published study comparing cDNA microarray data from 56 NFPanNETs with data from pancreatic NICs,[33] we randomly selected 15 NFPanNET samples from this microarray data set for cross-validation and observed that CDK4 expression was the highest among all samples (average, 6.9-fold vs pancreatic NICs) and Notch3 expression was lowest (average, 3.8-fold vs pancreatic NICs). Lef-1, CDK6, PDGFRB, and IGF2 also were overexpressed compared with their expression in pancreatic NICs (fold change: range, 3.8-fold to 4.9-fold).

DISCUSSION

The molecular mechanisms that give rise to NFPanNETs are complex and are not completely understood. Inactivating germline or somatic mutations in tumor-suppressor genes like *VHL* or *MEN1* contribute significantly to the tumorigenesis of NFPanNETs. However, additional events involved in proliferative and antiapoptotic signals and, in certain cases, evasion of the immune system and modification in the tumor microenvironment, are important in the initiation and/or progression of NFPanNETs. Proliferative and antiapoptotic signals are probably genotype-specific, as demonstrated in the current study, and arise from aberrant regulation of signal-transduction/growth (the phosphoinositide 3-kinase/protein kinase B [PI3K/AKT]), hypoxia/angiogenesis (VHL mutation), cell-cycle progression (down-regulation of CDK inhibitors), and/or genome-stabilization pathways.
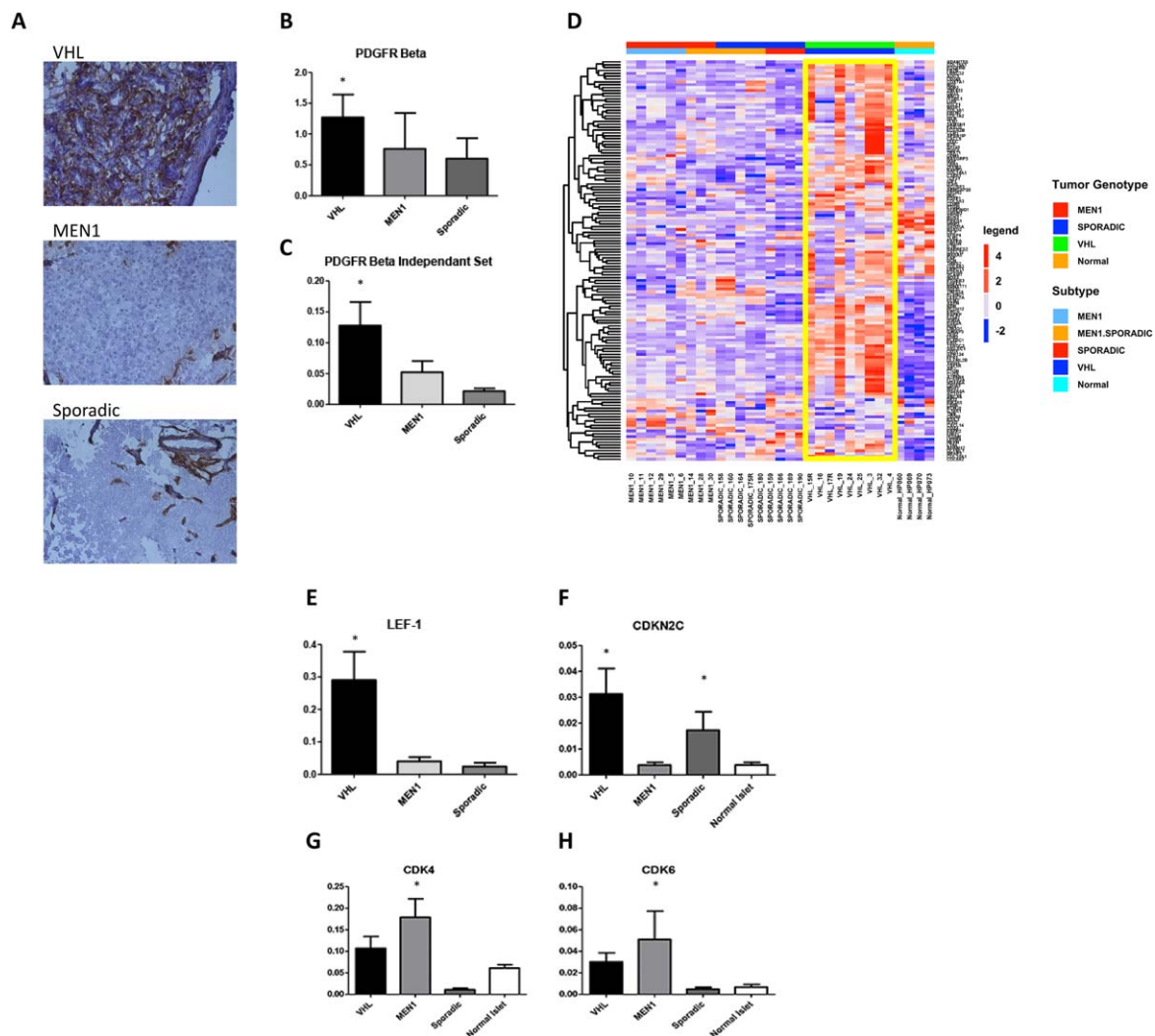
Figure 6. (A) Immunohistochemical analysis of platelet-derived growth factor receptor β (PDGFRB) in von Hippel-Lindau disease (VHL), multiple endocrine neoplasia type 1(MEN1), and sporadic pancreatic neuroectodermal tumors (PanNETs) reveals significantly increased expression in VHL PanNET cells ($P < .05$). (B) Reverse transcriptase-quantitative polymerase chain reaction (RT-qPCR) analysis of PDGFRB expression confirms the microarray analysis and indicates significantly increased messenger RNA (mRNA) levels in the initial cohort. (C) Independent RT-qPCR validation of PDGFRB expression is illustrated in a separate set of 19 nonfunctioning PanNETs (NFPanNETs) and 4 normal islet cell samples ($P < .05$). (D). The "Estimation of Stromal and Immune Cells in Malignant Tumors Using Expression Data" (ESTIMATE) gene signature model confirms an increased stromal signature in VHL PanNETs (yellow box). (E-H) RT-qPCR expression analysis reveals (E) overexpression of the transcription factor lymphoid enhancer-binding factor-1 (LEF1) in VHL NFPanNETs compared with sporadic and MEN1-associated NFPanNETs; (F) overexpression of the cyclin-dependent kinase 4 (CDK4)/CDK6 inhibitor 2C (CDKN2C) in MEN1-associated NFPanNETs compared with sporadic ($P = .06$) and VHL-associated ($P = .02$) NFPanNETs; (G) overexpression of CDK4 in MEN1-associated NFPanNETs compared with sporadic NFPanNETs ($P = .0009$) and normal islet cells ($P = .05$); and (H) overexpression of CDK6 in MEN1-associated NFPanNETs compared with sporadic NFPanNETs ($P = .05$). Asterisk indicates statistically significant ($p < .05$).

Previous studies investigating transcriptional alterations in PanNETs have mostly focused on comparing *benign* versus *malignant* PanNETs, defining these categories according to the absence or presence of metastatic disease.[27,29,34,35] Most of those studies also comprised relatively small samples sizes and/or heterogenous PanNET cohorts, including functioning and nonfunctioning tumors, or used normal pancreatic tissues as a

control.[29,34,35] The objective of our current analysis was to identify transcriptional alterations based on tumor genotype. Indeed, we discovered a subset of sporadic tumors that cluster with MEN1 tumors, revealing an additional way to classify tumors according to gene-expression phenotypes. In addition, our sample selection was purposely designed to be as homogenous as possible to uncover differences in pathways according to tumor

genotype rather than differences in stage-dependent tumor biology. We did not observe any statistically significant differential gene expression across tumor grades or samples with lymph node metastases. This is likely because most tumors had a low Ki-67 index within the grade 2 group, and the rate of lymph node metastases was too low in each of the subgroup to perform an adequately powered analysis. However, we believe that, by choosing a homogenous group of stage I and II NFPanNETs for each genotype, we uncovered transcriptional alterations that may occur at earlier stages in NFPanNET tumorigenesis.

Mutations in the tumor-suppressor *VHL* gene cause E3 ubiquitin ligase inactivity and subsequent upregulation of the hypoxia-inducible factor 1α (HIF1α) protein by inhibiting its degradation.[17] HIF1α is a transcription factor that induces the expression of several angiogenesis-related factor, as demonstrated in the current study, but also induces the expression of genes that promote macrophage and neutrophil energy generation, inflammatory and bactericidal activities, and cell survival.[17,36] The exact mechanisms by which VHL-mutated cells influence the immune system response are complex and poorly understood. However, some data suggest that the proangiogenesis state of VHL-mutated cells is central for immune response evasion of tumor cells. It has been demonstrated that the high proangiogenic status of clear cell renal cell cancers (RCCs), which commonly have VHL mutations, is associated with an accumulation of regulatory T cells and myeloid-derived suppressor cells in the local tumor microenvironment, particularly in the tumor invasion zone.[37] This might allow cells to evade immune surveillance, thereby promoting disease progression. Another recent study in RCC also has suggested that VHL-dependent alterations of the RCC secretome modulate T-cell activation by negatively interfering with T-cell proliferation and cytokine secretion.[29] Vascular endothelial growth factor (VEGF) overexpression has also been directly linked to immunosuppression by inhibiting the maturation of dendritic cells through a nuclear factor κB-dependent pathway (mediated by VEGFR-1 signaling) and to promoting the induction of regulatory CD4-positive/CD25-positive T cells within the tumor microenvironment.[38] Finally, increased adenosine concentrations observed in VHL-mutated cells is involved in impaired T-cell–mediated tumor rejection and supports tumor angiogenesis.[39,40]

PDGFRB is a tyrosine kinase inhibitor involved in angiogenesis, autocrine stimulation of tumor cells, and regulation of interstitial fluid pressure.[41-43] Only a few reports have analyzed the expression of *PDGFRB* in PanNETs, and all indicated that functioning PanNETs and NFPanNETs overexpress PDGFRB mRNA and protein.[35,41,44] In the current study, we demonstrated that the VHL NFPanNET genotype expresses the highest PDGFRB mRNA and protein levels compared with the MEN1 and sporadic genotypes and that PDGFRB protein staining is mostly positive in the VHL stroma. PDGFRB in tumor stroma is important for regulating interstitial fluid pressure, and inhibition of this protein may allow for greater uptake of other chemotherapy drugs.[43] Thus, we propose that NFPanNETs with alterations in the *VHL* promoter or mutations in the *VHL* gene may be particularly susceptible to PDGFRB antagonist treatment.

Because the tyrosine kinase inhibitors currently used for treatment of advanced PanNETs can be associated with the development of resistance over time, a combination of antiangiogenic and immune-based treatment could be beneficial in tumors that express high levels of angiogenic and immune infiltrating cells. Therefore, based on the current results, we believe that VHL-associated, locally advanced, and metastatic NFPanNETs may be especially good candidate for such combination therapies.

Singhi and colleagues analyzed the expression of LEF1 in pancreatic neoplasms and observed no expression in 44 well differentiated neuroendocrine tumors.[45] This contradicts our findings. It is unclear whether the PanNET samples studied were all sporadic and had no alterations in the *VHL* gene or VHL expression levels. If it is further confirmed that the transcription factor LEF1 is upregulated only in VHL NFPanNETs, then it potentially could be targeted by the currently available small-molecule inhibitors used in chronic lymphocytic leukemia.[46]

CDK inhibitor 1B (CDKN1B [p27^{Kip1}]) is an enzyme inhibitor, and we observed that it was underexpressed in the MEN1 NFPanNET genotype. CDKN1B is considered a tumor suppressor because it functions as a cell-cycle regulator, by in part preventing the activation of the cyclin D-CDK4 complex. Its inactivation can be accomplished post-transcription by the activation of several pathways, including the Ras-mitogen–activated protein kinase pathway, which is upregulated in MEN1 NFPanNETs, as was previously reported.[47]

In this study, we also demonstrated that CDK4 and CDK6 gene expression was higher in the MEN1 NFPanNET genotype. Tang and associates analyzed the

expression of CDK4 and CDK6 in functioning PanNETs and NFPanNETs and reported high CDK4 expression levels and increased copy numbers of CDK4 and CDK6. They also observed that the human PanNET cell line QGP1 was inhibited in a xenograft mouse model by the CDK4/CDK6 inhibitor PD0332991.[48] In another study, knockdown of CDK6 enhanced glioma sensitivity to the chemotherapeutic temozolomide, which has demonstrated effectiveness in treating PanNETs.[49,50] Inhibitors of CDK6 are currently in clinical trials for other malignancies; therefore, understanding which subset of NFPanNETs could benefit from CDK4/CDK6 inhibition and potentially from enhancing temozolomide efficacy with CDK6 inhibitors would be of interest and should be investigated further.

The current study has several limitations. We used human islets cells for some of the comparisons, and these cells were not sorted to distinguish the specific cell type population. This may have influenced the results from comparing NFPanNETs with NICs, because it is generally believed that NFPanNETs originate from a single cell type. Newer methods to isolate single-cell populations have recently been described and could be applied in the future.[51] Furthermore, although we confirmed the overexpression of LEF1, CDK4, CDK6, NOTCH3, RYR3, and IGF2 in an independent cohort of NFPanNETs, we cannot reliably determine that these genes can segregate NFPanNETs by genotype, because this particular validation set does not have data on mutations in the *MEN1* or *VHL* genes. Additional future studies will be needed for this purpose. Finally, although we validated highly differentially expressed genes that may have biologic significance and could be targeted for therapy at the protein level (such as PDGFRB), we cannot be certain that this applies to all of the differentially expressed genes identified in the current study.

In summary, we have demonstrated genotype-specific differences in mRNA expression patterns in sporadic NFPanNETs, VHL-associated NFPanNETs, and MEN1-associated NFPanNETs; and the results suggest that genotype-specific and subtype-specific activation of pathways may contribute to NFPanNET tumorigenesis. These findings implicate specific genes and pathways that could be exploited to identify new diagnostic or therapeutic pathways and allow for subtype-specific treatments of NFPanNETs in the future.

FUNDING SUPPORT

CONFLICT OF INTEREST DISCLOSURES

Ralph H. Hruban reports royalties for the discovery of "partner and localizer of BRCA2" (PalB2) and support for participation as a board member in a relationship overseen by Johns Hopkins University School of Medicine. The remaining authors made no disclosures.

AUTHOR CONTRIBUTIONS

Xavier M. Keutgen: Experiment design and performance and writing–initial draft and editing. **Suresh Kumar**: Experiment design and performance. **Sudheer Gara**: Experiment design and performance. **Myriem Boufraqech**: Experiment design and performance. **Sunita Agarwal**: Experiment design and performance. **Ralph H. Hruban**: Statistical analysis and writing–initial draft and editing. **Naris Nilubol**: Writing–initial draft and editing. **Martha Quezado**: Experiment design and performance. **Richard Finney**: Statistical analysis. **Maggie Cam**: Statistical analysis and writing–initial draft and editing. **Electron Kebebew**: Writing–initial draft and editing.

REFERENCES

1. Halfdanarson TR, Rubin J, Farnell MB, Grant CS, Petersen GM. Pancreatic endocrine neoplasms: epidemiology and prognosis of pancreatic endocrine tumors. *Endocrine Relat Cancer*. 2008;15:409-427.

2. Bilimoria KY, Tomlinson JS, Merkow RP, et al. Clinicopathologic features and treatment trends of pancreatic neuroendocrine tumors: analysis of 9,821 patients. *J Gastrointest Surg*. 2007;11:1460-1467; discussion 1467-1469.

3. Horton WA, Wong V, Eldridge R. Von Hippel-Lindau disease: clinical and pathological manifestations in 9 families with 50 affected members. *Arch Intern Med*. 1976;136:769-777.

4. Keutgen XM, Hammel P, Choyke PL, Libutti SK, Jonasch E, Kebebew E. Evaluation and management of pancreatic lesions in patients with von Hippel-Lindau disease. *Nat Rev Clin Oncol*. 2016; 13:537-549.

5. Kloppel G, Perren A, Heitz PU. The gastroenteropancreatic neuroendocrine cell system and its tumors: the WHO classification. *Ann N Y Acad Sci*. 2004;1014:13-27.

6. Neychev V, Sadowski SM, Zhu J, et al. Neuroendocrine tumor of the pancreas as a manifestation of Cowden syndrome: a case report. *J Clin Endocrinol Metab*. 2016;101:353-358.

7. Sadowski SM, Triponez F. Management of pancreatic neuroendocrine tumors in patients with MEN 1. *Gland Surg*. 2015;4:63-68.

8. de Mestier L, Gaujoux S, Cros J, et al. Long-term prognosis of resected pancreatic neuroendocrine tumors in von Hippel-Lindau disease is favorable and not influenced by small tumors left in place. *Ann Surg*. 2015;262:384-388.

9. Blansfield JA, Choyke L, Morita SY, et al. Clinical, genetic and radiographic analysis of 108 patients with von Hippel-Lindau disease (VHL) manifested by pancreatic neuroendocrine neoplasms (PNETs). *Surgery*. 2007;142:814-818; discussion 818.e1-818.e2.

10. Charlesworth M, Verbeke CS, Falk GA, Walsh M, Smith AM, Morris-Stiff G. Pancreatic lesions in von Hippel-Lindau disease? A systematic review and meta-synthesis of the literature. *J Gastrointest Surg*. 2012;16:1422-1428.

11. Hammel PR, Vilgrain V, Terris B, et al. Pancreatic involvement in von Hippel-Lindau disease. The Groupe Francophone d'Etude de la Maladie de von Hippel-Lindau. *Gastroenterology*. 2000;119:1087-1095.

12. Libutti SK, Choyke PL, Bartlett DL, et al. Pancreatic neuroendocrine tumors associated with von Hippel Lindau disease: diagnostic and management recommendations. *Surgery*. 1998;124:1153-1159.

13. Jiao Y, Shi C, Edil BH, et al. DAXX/ATRX, MEN1, and mTOR pathway genes are frequently altered in pancreatic neuroendocrine tumors. *Science*. 2011;331:1199-1203.

14. Dong M, Phan AT, Yao JC. New strategies for advanced neuroendocrine tumors in the era of targeted therapy. *Clin Cancer Res*. 2012;18:1830-1836.

15. Schmitt AM, Schmid S, Rudolph T, et al. VHL inactivation is an important pathway for the development of malignant sporadic pancreatic endocrine tumors. *Endocrine Relat Cancer*. 2009;16:1219-1227.

16. Zhang J, Francois R, Iyer R, Seshadri M, Zajac-Kaye M, Hochwald SN. Current understanding of the molecular biology of pancreatic neuroendocrine tumors. *J Natl Cancer Inst*. 2013;105:1005-1017.

17. Lonser RR, Glenn GM, Walther M, et al. von Hippel-Lindau disease. *Lancet*. 2003;361:2059-2067.

18. Ritchie ME, Phipson B, Wu D, et al. limma powers differential expression analyses for RNA-sequencing and microarray studies [serial online]. *Nucleic Acids Res*. 2015;43:e47.

19. Wilkerson MD, Hayes DN. ConsensusClusterPlus: a class discovery tool with confidence assessments and item tracking. *Bioinformatics*. 2010;26:1572-1573.

20. Larsson C, Calender A, Grimmond S, et al. Molecular tools for presymptomatic testing in multiple endocrine neoplasia type 1. *J Intern Med*. 1995;238:239-244.

21. Manickam P, Guru SC, Debelenko LV, et al. Eighteen new polymorphic markers in the multiple endocrine neoplasia type 1 (MEN1) region. *Hum Genet*. 1997;101:102-108.

22. Godin-Heymann N, Brabetz S, Murillo MM, et al. Tumour-suppression function of KLF12 through regulation of anoikis. *Oncogene*. 2016;35:3324-3334.

23. Zhou HQ, Chen QC, Qiu ZT, Tan WL, Mo CQ, Gao SW. Integrative microRNA-mRNA and protein-protein interaction analysis in pancreatic neuroendocrine tumors. *Eur Rev Med Pharmacol Sci*. 2016;20:2842-2852.

24. Merrill MJ, Edwards NA, Lonser RR. Notch receptor and effector expression in von Hippel-Lindau disease-associated central nervous system hemangioblastomas. *J Neurosurg*. 2011;115:512-517.

25. van Adrichem RC, de Herder WW, Kamp K, et al. Effects of somatostatin analogs and dopamine agonists on insulin-like growth factor 2-induced insulin receptor isoform A activation by gastroenteropancreatic neuroendocrine tumor cells. *Neuroendocrinology*. 2016;103:815-825.

26. Johnson JD, Kuang S, Misler S, Polonsky KS. Ryanodine receptors in human pancreatic beta cells: localization and effects on insulin secretion. *FASEB J*. 2004;18:878-880.

27. Missiaglia E, Dalai I, Barbi S, et al. Pancreatic endocrine tumors: expression profiling evidences a role for AKT-mTOR pathway. *J Clin Oncol*. 2010;28:245-255.

28. Erlic Z, Ploeckinger U, Cascon A, et al. Systematic comparison of sporadic and syndromic pancreatic islet cell tumors. *Endocrine Relat Cancer*. 2010;17:875-883.

29. Wang DD, Liu ZW, Han MM, et al. Microarray based analysis of gene expression patterns in pancreatic neuroendocrine tumors. *Eur Rev Med Pharmacol Sci*. 2015;19:3367-3374.

30. Lopez-Avalos MD, Duvivier-Kali VF, Xu G, Bonner-Weir S, Sharma A, Weir GC. Evidence for a role of the ubiquitin-proteasome pathway in pancreatic islets. *Diabetes*. 2006;55:1223-1231.

31. Speisky D, Duces A, Bieche I, et al. Molecular profiling of pancreatic neuroendocrine tumors in sporadic and von Hippel-Lindau patients. *Clin Cancer Res*. 2012;18:2838-2849.

32. Yoshihara K, Shahmoradgoli M, Martinez E, et al. Inferring tumour purity and stromal and immune cell admixture from expression data [serial online]. *Nat Commun*. 2013;4:2612.

33. Sadanandam A, Wullschleger S, Lyssiotis CA, et al. A cross-species analysis in pancreatic neuroendocrine tumors reveals molecular subtypes with distinctive clinical, metastatic, developmental, and metabolic characteristics. *Cancer Discov*. 2015;5:1296-1313.

34. Bloomston M, Durkin A, Yang I, et al. Identification of molecular markers specific for pancreatic neuroendocrine tumors by genetic profiling of core biopsies. Ann Surg. *Oncol*. 2004;11:413-419.

35. Duerr EM, Mizukami Y, Ng A, et al. Defining molecular classifications and targets in gastroenteropancreatic neuroendocrine tumors through DNA microarray analysis. *Endocrine Relat Cancer*. 2008;15:243-256.

36. Walmsley SR, McGovern NN, Whyte MK, Chilvers ER. The HIF/VHL pathway: from oxygen sensing to innate immunity. *Am J Respir Cell Mol Biol*. 2008;38:251-255.

37. Ning H, Shao QQ, Ding KJ, et al. Tumor-infiltrating regulatory T cells are positively correlated with angiogenic status in renal cell carcinoma. *Chin Med J (Engl)*. 2012;125:2120-2125.

38. Tartour E, Pere H, Maillere B, et al. Angiogenesis and immunity: a bidirectional link potentially relevant for the monitoring of antiangiogenic therapy and the development of novel therapeutic combination with immunotherapy. *Cancer Metastasis Rev*. 2011;30:83-95.

39. Mediavilla-Varela M, Luddy K, Noyes D, et al. Antagonism of adenosine A2A receptor expressed by lung adenocarcinoma tumor cells and cancer associated fibroblasts inhibits their growth. *Cancer Biol Ther*. 2013;14:860-868.

40. Cuperlovic-Culf M, Cormier K, Touaibia M, et al. ^{1}H NMR metabolomics analysis of renal cell carcinoma cells: Effect of VHL inactivation on metabolism. *Int J Cancer*. 2016;138:2439-2349.

41. Fjallskog ML, Hessman O, Eriksson B, Janson ET. Upregulated expression of PDGF receptor beta in endocrine pancreatic tumors and metastases compared to normal endocrine pancreas. *Acta Oncol*. 2007;46:741-746.

42. McGary EC, Weber K, Mills L, et al. Inhibition of platelet-derived growth factor-mediated proliferation of osteosarcoma cells by the novel tyrosine kinase inhibitor STI571. *Clin Cancer Res*. 2002;8:3584-3591.

43. Pietras K, Stumm M, Hubert M, et al. STI571 enhances the therapeutic index of epothilone B by a tumor-selective increase of drug uptake. *Clin Cancer Res*. 2003;9(10 pt 1):3779-3787.

44. Fjallskog ML, Lejonklou MH, Oberg KE, Eriksson BK, Janson ET. Expression of molecular targets for tyrosine kinase receptor antagonists in malignant endocrine pancreatic tumors. *Clin Cancer Res*. 2003;9:1469-1473.

45. Singhi AD, Lilo M, Hruban RH, Cressman KL, Fuhrer K, Seethala RR. Overexpression of lymphoid enhancer-binding factor 1 (LEF1) in solid-pseudopapillary neoplasms of the pancreas. *Mode Pathol*. 2014;27:1355-1363.

46. Gandhirajan RK, Staib PA, Minke K, et al. Small molecule inhibitors of Wnt/beta-catenin/lef-1 signaling induces apoptosis in chronic lymphocytic leukemia cells in vitro and in vivo. *Neoplasia*. 2010;12:326-335.

47. Chu IM, Hengst L, Slingerland JM. The Cdk inhibitor p27 in human cancer: prognostic potential and relevance to anticancer therapy. *Nat Rev Cancer*. 2008;8:253-267.

48. Tang LH, Contractor T, Clausen R, et al. Attenuation of the retinoblastoma pathway in pancreatic neuroendocrine tumors due to increased cdk4/cdk6. *Clin Cancer Res*. 2012;18:4612-4620.

49. Li B, He H, Tao BB, et al. Knockdown of CDK6 enhances glioma sensitivity to chemotherapy. *Oncol Rep*. 2012;28:909-914.

50. Peixoto RD, Noonan KL, Pavlovich P, Kennecke HF, Lim HJ. Outcomes of patients treated with capecitabine and temozolamide for advanced pancreatic neuroendocrine tumors (PNETs) and non-PNETs. *J Gastrointest Oncol*. 2014;5:247-252.

51. Li J, Klughammer J, Farlik M, et al. Single-cell transcriptomes reveal characteristic features of human pancreatic islet cell types. *EMBO Rep*. 2016;17:178-187.